NEURO-ONCOLOGY

Tumor invasion after treatment of glioblastoma with bevacizumab: radiographic and pathologic correlation in humans and mice

John F. de Groot, Gregory Fuller, Ashok J. Kumar, Yuji Piao, Karina Eterovic, Yongjie Ji, and Charles A. Conrad

Brain Tumor Center (J.F.G., Y.P., K.E., Y.J., C.A.C.); Department of Neuropathology (G.F.); Department of Neuroradiology (A.J.K.), The University of Texas M. D. Anderson Cancer Center, Houston, Texas

Patients with recurrent malignant glioma treated with bevacizumab, a monoclonal antibody to vascular endothelial growth factor (VEGF), alone or in combination with irinotecan have had impressive reductions in MRI contrast enhancement and vasogenic edema. Responses to this regimen, as defined by a decrease in contrast enhancement, have led to significant improvements in progression-free survival rates but not in overall survival duration. Some patients for whom this treatment regimen fails have an uncharacteristic pattern of tumor progression, which can be observed radiographically as an increase in hyperintensity on T2-weighted or fluid-attenuated inverse recovery (FLAIR) MRI. To date, there have been no reports of paired correlations between radiographic results and histopathologic findings describing the features of this aggressive tumor phenotype. In this study, we correlate such findings for 3 illustrative cases of gliomas that demonstrated an apparent phenotypic shift to a predominantly infiltrative pattern of tumor progression after treatment with bevacizumab. Pathologic examination of abnormal FLAIR areas on MRI revealed infiltrative tumor with areas of thin-walled blood vessels, suggesting vascular "normalization," which was uncharacteristically adjacent to regions of necrosis. High levels of insulin-like growth factor binding protein-2 and matrix metalloprotease-2 expression were seen within the infiltrating tumor. In an attempt to better understand this infiltrative phenotype associated with anti-VEGF therapy, we forced a highly angiogenic, noninvasive orthotopic U87 xenograft tumor to become infiltrative by treating the mice with bevacizumab. This model mimicked many of the histopathologic findings from the human cases and will augment the discovery of alternative or additive therapies to prevent this type of tumor recurrence in clinical practice.

Keywords: bevacizumab, glioblastoma, invasion, matrix metalloproteinases, VEGF

The prognosis of patients with malignant gliomas remains poor despite decades of basic and clinical research. Median survival durations are approximately 12–14 months for patients diagnosed with glioblastoma[1,2] and 3–5 years for patients diagnosed with anaplastic astrocytoma.[3] Because high-grade gliomas are highly angiogenic, there is a convincing rationale for targeting the tumor vasculature. High-grade gliomas secrete large amounts of vascular endothelial growth factor (VEGF), which acts in a paracrine manner to promote endothelial cell proliferation, survival, and migration.[4] Inhibiting VEGF is an effective anticancer therapy,[5–7] and several clinical trials have demonstrated a high response rate and improvements in progression-free survival rate in patients with recurrent glioblastoma treated with bevacizumab, with or without irinotecan,[8–10] compared with outcomes for historical controls.[2] VEGF receptor inhibitors also have activity against glioblastoma, as demonstrated in a recent study of the pan-VEGF receptor tyrosine kinase inhibitor cediranib (also called AZD2171 or Recentin, AstraZeneca), in which radiographic response rates were approximately 50% and the 6-month

progression-free survival rate was 27%.[11] Surprisingly, VEGF and VEGF receptor inhibitors have resulted in little improvement in overall survival duration,[12] and tumors that progress during bevacizumab therapy are highly resistant to subsequent therapies.[13]

Blocking VEGF has been shown to prune abnormal tumor blood vessels and "normalize" the remaining vasculature.[14] Although vascular permeability is decreased within the tumor, it has been hypothesized that vascular normalization temporarily improves oxygen and drug delivery to the tumor,[14–16] thereby improving treatment efficacy. Reduced vascular permeability has several clinical benefits, including decreasing cerebral edema and accompanying neurologic symptoms, allowing patients to minimize corticosteroid use.[11] However, changes in vascular permeability measured through dynamic contrast-enhanced MRI do not predict the long-term outcome of patients who receive bevacizumab,[17] suggesting that decreases in permeability are necessary but not sufficient to produce long-term responses. Glioblastoma rapidly adapts to anti-VEGF therapy, leading to rapid tumor progression without improvement in overall survival.

The purpose of this study was to investigate the phenotypic change in radiographic tumor progression that has been observed in some patients receiving bevacizumab. We describe 3 patients who, during bevacizumab therapy, developed infiltrative lesions visible by MRI. Tumor tissue was obtained from these patients during treatment and, for the first time, we present data that pair imaging features seen on MRI with histopathologic findings. We found a decrease in tumor vascularity and lack of glomeruloid endothelial proliferation within the tumor. Blood vessels with walls of a single layer of endothelial cells were present, consistent with vascular normalization. Interestingly, these more normal-appearing vessels were found immediately adjacent to the areas of tumor necrosis. At the leading edge of the tumor, we were not able to demonstrate perivascular tumor invasion. To better understand the tumor biology of progression during, or "escape" from, anti-VEGF therapy, we further substantiated our findings in a murine orthotopic xenograft model derived from U87 glioma cells. We found that prolonged anti-VEGF treatment led to tumor invasion through perivascular and subpial tumor invasion. These findings will augment the discovery of potential mechanisms of tumor invasion and aid in the development of drug combinations to treat or prevent this phenotypic shift.

Patients and Methods

Patients

We identified 3 patients for whom a pattern of non-enhancing (non–contrast-enhancing) tumor infiltration was the mechanism of tumor progression during bevacizumab treatment for biopsy-proven recurrent disease. These 3 patients were selected for careful neuroradiologic review of all MRI sequences by one of our neuroradiologists (A.J.K.). Using MRI studies, the area of the largest lesion of progressive disease at the level of the maximum bidimensional measurement was determined for each patient. Both gadolinium contrast-enhanced images and noncontrast fluid-attenuated inverse recovery (FLAIR) sequences were used for these measurements. The change in area from that measured on the pretreatment MRI image or on the last stable MRI image available was recorded and was expressed as a percentage change, as described previously.[18] These patients were determined to have had bidimensional measurement increases of greater than 25% at the time of treatment failure. In all 3 cases, more than 6 months had passed between completing radiation therapy and starting bevacizumab. The interval between the last dose of bevacizumab and the surgery to remove the recurrent tumor was less than 30 days in all 3 cases. For this study, informed consent was obtained for patients and was approved by the University of Texas M. D. Anderson Cancer Center Institutional Review Board.

Mouse Xenograft Orthotopic Models

All animal experiments utilized the U87 glioma cell line, which was obtained from the American Type Culture Collection. U87 tumor cells were implanted into nude mice by the screw-guided method as described previously.[19] Beginning 5 days after tumor implantation, animals were treated with bevacizumab at 10 mg/kg i.p. twice weekly or IgG at 10 mg/kg i.p. twice weekly (as a control). Animals were observed closely for signs of clinical deterioration, at which time they were killed in accordance with the regulations and guidelines of the Institutional Animal Care and Use Committee (IACUC). All experiments were approved by the animal care and use committee of the M. D. Anderson Cancer Center. After euthanasia, tumors were extracted, fixed in formalin, and then paraffin embedded.

Immunohistochemistry

Immunohistochemical analysis of total insulin-like growth factor binding protein-2 (IGFBP2), matrix metalloprotease-2 (MMP2), carbonic anhydrase IX (CA9), and factor VIII was performed on paraffin-embedded, formalin-fixed xenograft and human tumor tissue. Briefly, 5-mm-thick sections were mounted on positively charged slides, deparaffinized, and rehydrated in phosphate-buffered saline (PBS). Endogenous peroxidase activity was blocked with 3% hydrogen peroxide in PBS/0.05% Tween 20 for 20 minutes. Sections were then washed in PBS and blocked for 20 minutes in the appropriate serum from the same species as the secondary antibody, diluted to 10% in PBS. Microwave antigen retrieval was performed by placing the slides in 50 mM citrate buffer (pH 6.0) and microwaving for 12 minutes at full power and 10 minutes at 20% power, followed by cooling for 15 minutes and washing in PBS 2–3 times for 5 minutes

each. Primary antibodies, diluted in PBS/10% serum, were applied to the sections in a humid chamber overnight at 48°C. Secondary antibodies were applied using the Dako EnVision kit (Carpinteria, CA) according to the manufacturer's instructions. Detection of bound secondary antibody was performed with diaminobenzidine. Sections were then counterstained with light hematoxylin and mounted. The primary antibodies used were as follows: IGFBP2 (Santa Cruz Biotechnology, Santa Cruz, CA), factor VIII (catalog number A0082, Dako), CA9 (Novus Biologicals, Littleton, CO), and MMP2 (sc-6838, Santa Cruz Biotechnology).

Results

Human Radiographic Imaging and Pathologic Correlation

Case 1. The first patient was a 31-year-old man who was diagnosed with a right posterior frontal–anterior parietal lobe glioblastoma followed by chemoradiation with concurrent temozolomide followed by adjuvant temozolomide. The patient had rapid progression and underwent a second surgical resection. After surgery and documentation of tumor progression, he was enrolled onto protocol to receive temozolomide and Hominex (a methionine-restricted diet). The patient received 2 cycles of treatment and then, when disease progressed, underwent a third surgical resection. He then received off-protocol 6-thioguanine, lomustine, capecitabine, chloroquine, imatinib, and hydroxyurea and did well for 13 months until a recurrence was noted in April 2006.

At this time, the patient began treatment with bevacizumab and irinotecan and had a complete response, which lasted from April 2006 until March 2007. The initial response is shown in Fig. 1 (compare panels A and B, taken before bevacizumab treatment, with panels C and D, taken 3 months later after bevacizumab treatment). There were marked decreases in vascular permeability (visualized as enhancement) on the contrast-enhanced MRI images and in vasogenic edema on the FLAIR images. The patient then experienced clinical decline consisting of increased left-sided weakness, daytime fatigue, and a decrease in mobility. The MRI scans dated March 1, 2007 (Fig. 1E), show that the lack of vascular permeability had persisted (there was no evidence of contrast enhancement); however, there was an increase in the amount of infiltrative disease (Fig. 1F, arrows), with swollen infiltrative gyri. The patient's therapy was discontinued, and a
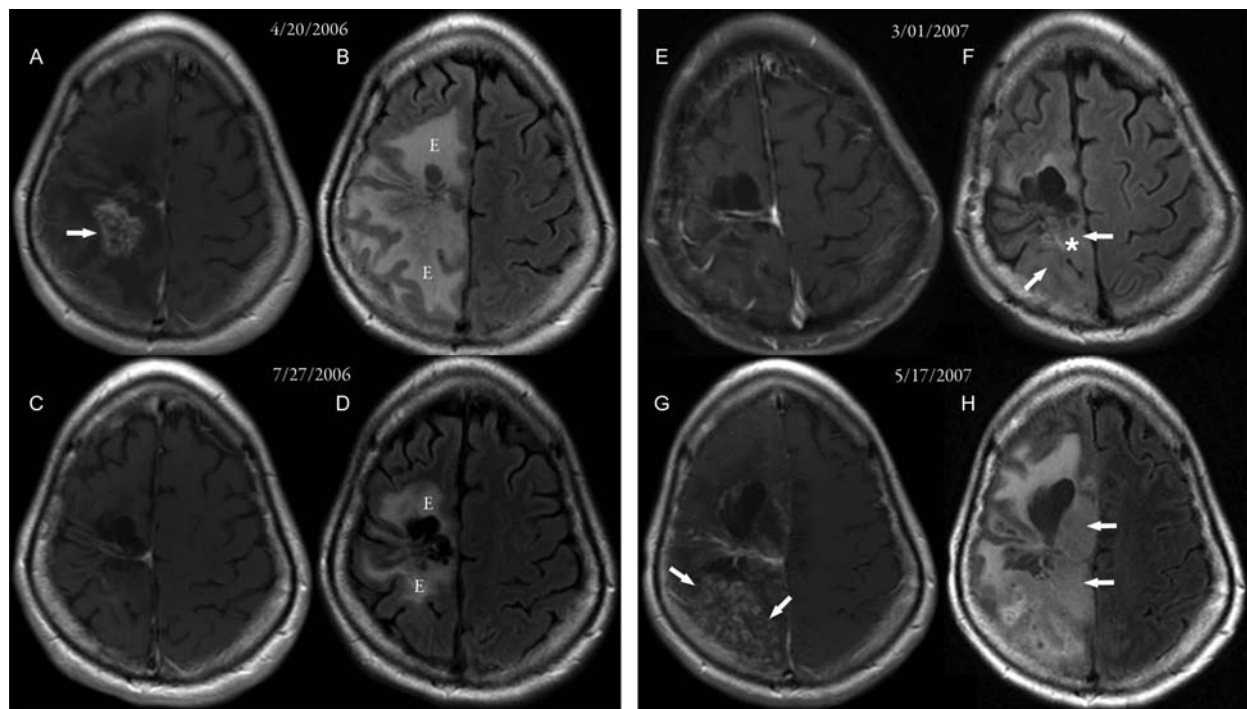

Fig. 1. MR images from case 1. (A, C, E, and G) Postcontrast axial T1-weighted MR images. (B, D, F, and H) FLAIR MR images. (A and B) Images taken 18 months after 2 surgeries, radiation therapy, and chemotherapy for recurrent glioblastoma. An inhomogeneously enhancing area with necrosis (arrow in A) was seen posterior to the right frontal lobe surgical cavity, with a large area of surrounding edema ("E" in B). (C and D) Images taken 3 months after beginning bevacizumab therapy. The enhancement posterior to the right frontal lobe surgical cavity had disappeared, and there was a significant decrease in the surrounding edema ("E" in D). (E and F) Images taken 8 months after starting bevacizumab therapy. Subtle areas of nonenhancing FLAIR changes (arrows in F) were seen posterior to the surgical cavity, consistent with nonenhancing tumor. (G and H) Images taken approximately 2 months after stopping bevacizumab. Significant progression of nonenhancing tumor (arrows in H) and spotty areas of enhancing tumor (arrows in G) were seen. The approximate biopsy site is indicated by the white asterisk.

biopsy was performed on March 2, 2007; it demonstrated definite infiltrative glioma. The biopsy specimen taken from this nonenhancing tumor lacked significant vascular proliferation but was densely cellular. A repeat MRI scan approximately 2 months later, dated May 17, 2007, showed an increase in enhancement (Fig. 1G and H) with an increase in infiltrative bulky disease (arrows).

Case 2. The second patient was a 64-year-old man originally diagnosed with an anaplastic astrocytoma of the left frontal lobe in December 2004. After surgery, he underwent chemoradiation with adjuvant temozolomide. He then was treated with multiple regimens, including thalidomide plus irinotecan and the combination of 6-thioguanine, lomustine, capecitabine, and chloroquine, but tumor progression occurred on this regimen. He started bevacizumab and irinotecan treatment and had a complete response, as demonstrated by the absence of contrast-enhancing tumor (compare Fig. 2A, taken April 20, 2006, before bevacizumab, and C, taken October 3, 2006, after bevacizumab). Vasogenic edema also improved (compare Fig. 2B and D). The patient had slow progression of his neurologic symptoms of fatigue, decreased memory, and loss of executive functions. The MRI scans dated January 8, 2007, demonstrate a lack of contrast enhancement (Fig. 2E), but a definite increase in the amount of non–contrast-enhancing infiltrative disease (Fig. 2F, arrows). A stereotactic biopsy on March 2, 2007, demonstrated areas of necrosis and viable diffuse infiltrative glioma.

Case 3. The third patient was a 19-year-old man who was diagnosed with a bifrontal glioblastoma. He was treated postoperatively with chemoradiation with concurrent temozolomide followed by temozolomide, thalidomide, and isotretinoin for a total of 12 cycles. An MRI scan revealed recurrent disease, so he was placed on a regimen of carboplatin plus bevacizumab. This patient had a dramatic improvement in the amount of contrast-enhancing tumor (arrows) (compare Fig. 3A, taken November 14, 2006, before bevacizumab, and C, a 2-month post-treatment follow-up scan taken January 16, 2007). In an MRI scan taken March 12, 2007, there was a lack of change in contrast enhancement (Fig. 3D and F, arrows) but an increase in the non–contrast-enhancing infiltrative component of the tumor. The patient's symptoms worsened, with increased abulia, fatigue, and headache. Surgical resection on May 21, 2007, revealed histopathologic evidence of infiltrative high-grade tumor.

Histologic and Molecular Tumor Analysis

Tumor tissue samples were taken from the 3 patients whose tumors progressed during anti-VEGF therapy. None of the cases had evidence of contrast-enhancing tumors on MRI scans taken at the time of biopsy or surgery. The tumor biopsies or surgical specimens were taken from areas of FLAIR abnormality seen on MRI, and in all cases histologic examination demonstrated abundant glioblastoma tumor cell infiltration. There was a striking lack of vascular proliferation with little evidence of vascular hyperproliferation and no evidence of glomeruloid vessels (Fig. 4A).

Comparison with the original surgical specimens revealed that both the first and third cases had abundant glomeruloid vascular proliferation consistent with the initial diagnosis of glioblastoma. The second case, originally diagnosed as a mixed anaplastic oligoastrocytoma, did not have vascular proliferation as would have been expected from the histologic diagnosis. However, at the time of bevacizumab treatment, the patient's clinical course had been rapid, there had been multiple recurrences, and the tumor was contrast enhancing, all suggesting that this patient's initial grade III tumor had transformed into a glioblastoma.

Single endothelial cell walled vessels were observed in all cases, consistent with the normalization of tumor vasculature after anti-VEGF therapy. Some of these normalized vessels were adjacent to areas of necrosis (Fig. 4A), a finding in sharp contrast to typical histologic observations, in which robust angiogenesis (mediated by VEGF secretion) is present around areas of tumor necrosis. Tumor progression and necrosis (Fig. 4A and B, white arrows) were occurring simultaneously with vascular normalization and vessel pruning. Areas identified by the neuropathologist as corresponding to the leading edge of the tumor did not show an increase in perivascular tumor infiltration (Fig. 4A, black arrows). The most abundant finding on histologic examination of the infiltrative tumor lesions was the typical invasion of glioma cells into neuropil (Fig. 5A, black arrows).

IGFBP2 has been identified as an important mediator of glioma cell invasion.[20] IGFBP2 (Fig. 4B, black arrows) expression was markedly elevated around regions of necrosis in all 3 cases (Fig. 4B, white arrows). Given the reported correlation between IGFBP2 and MMP2 expression,[20] we also evaluated MMP2 staining in bevacizumab-treated tumors. Very high levels of MMP2 expression were observed in all 3 cases (Fig. 4C, black arrows). In addition, we stained for factor VIII, which demonstrates endothelial cell proliferation. Less factor VIII staining was observed in the pathologic samples from our 3 patients treated with bevacizumab (Fig. 5A, white arrows). However, tumor tissue from bevacizumab-treated mice at terminal stages had very high levels of endothelial cell proliferation (Fig. 5C and D). Finally, evaluation of tumor levels of hypoxia was performed using the marker CA9. As shown in Fig. 5E and F, there were high levels of hypoxia surrounding areas of necrosis within the densely cellular tumor mass. Adjacent to these areas were the previously described single endothelial cell walled vessels, confirming our suspicion that prolonged, continuous antiangiogenic therapy can lead to increased tumor hypoxia. No CA9 staining was present within densely cellular regions of the initial diagnosis tumor samples (data not shown).
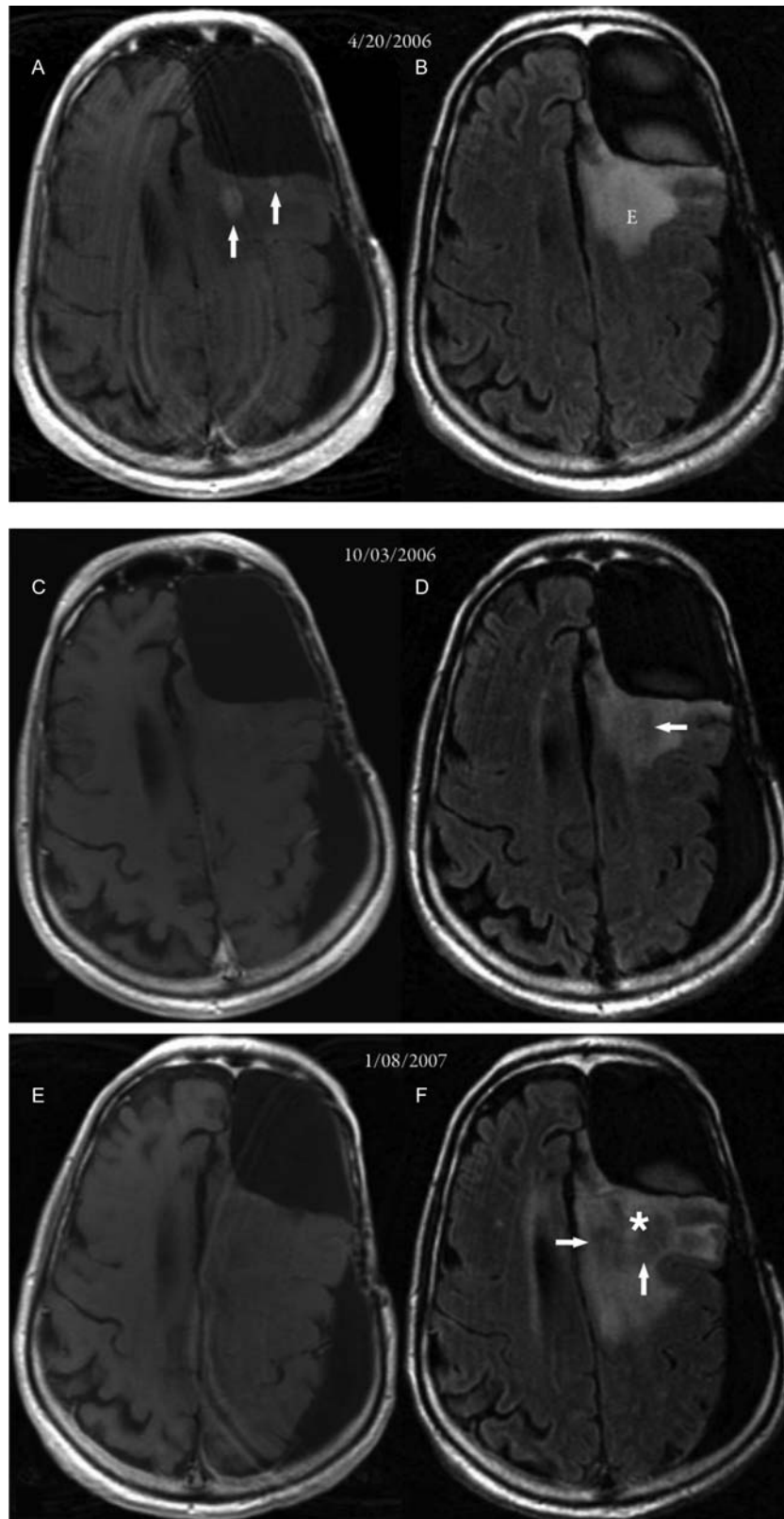
Fig. 2. MR images from case 2. (A, C, and E) Axial postcontrast T1-weighted MR images. (B, D, and F) Axial FLAIR MR images. (A and B) Images taken 1 year, 8 months after surgery, radiation therapy, and chemotherapy for an anaplastic mixed oligoastrocytoma in the left frontal lobe. Small enhancing areas (arrows in A) were seen posterior to the left frontal lobe surgical cavity, with surrounding edema ("E" in B). (C and D) Images taken 57 days after beginning bevacizumab therapy. Previously noted enhancing areas had disappeared, and there was a suggestion of nonenhancing tumor (arrow in D). (E and F) Images taken 95 days after starting bevacizumab therapy. An increase in the area of nonenhancing tumor (arrows in F) was evident, with an increase in edema. The approximate biopsy site is indicated by the white asterisk.
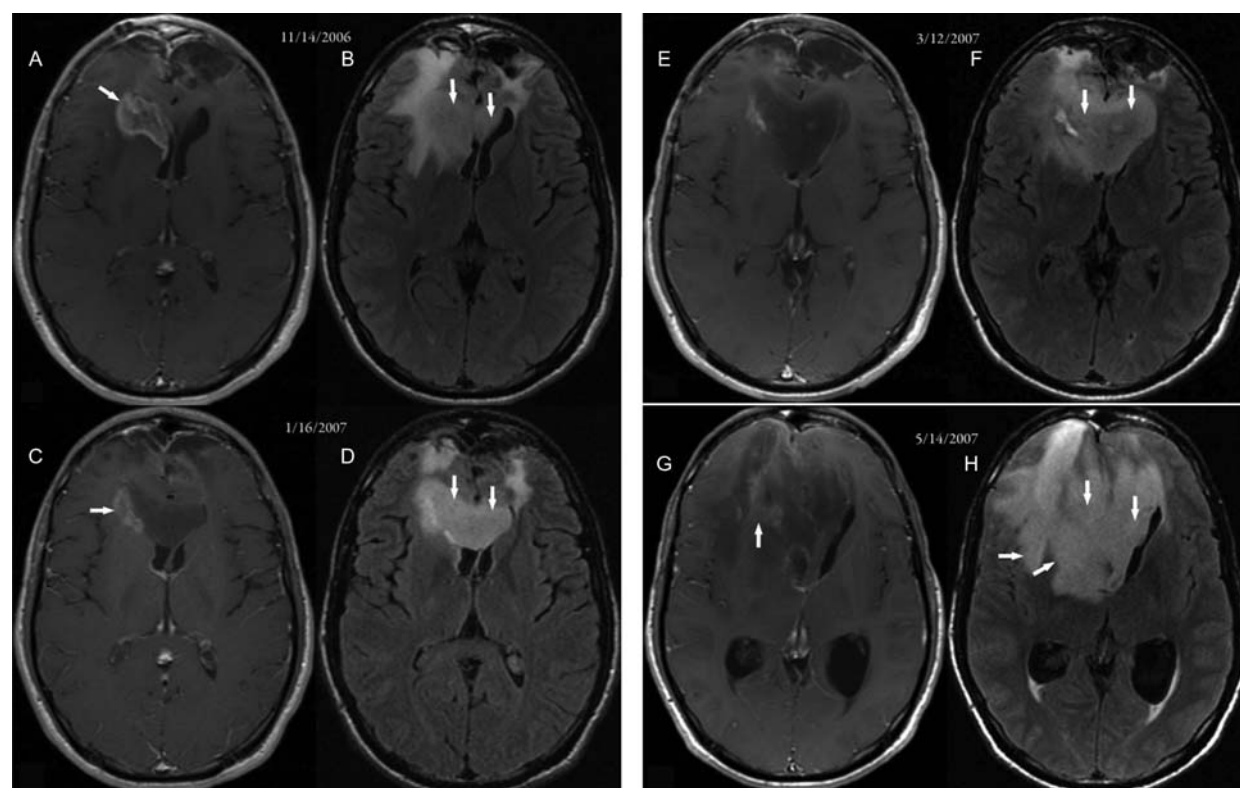
Fig. 3. MR images from case 3. (A, C, E, and G) Axial postcontrast T1-weighted MR images. (B, D, F, and H) FLAIR MR images. (A and B) Images taken 14 months after surgery, radiation therapy, and chemotherapy for bifrontal lobe glioblastoma that infiltrated across the genus of the corpus callosum. The enhancing area was seen in the right frontal lobe, capping and infiltrating the right frontal horn (arrow in A). Nonenhancing tumor within the corpus callosum (arrows in B) was better visualized in the FLAIR image. (C and D) Images taken 62 days after beginning bevacizumab therapy. The enhancing area within the right frontal lobe showed significant decrease (arrow in C), but the nonenhancing tumor showed progression (arrows in D). (E and F) Images taken 117 days after beginning bevacizumab therapy. The enhancing area within the right frontal lobe showed further decrease, but the nonenhancing tumor (arrows in F) showed progression. (G and H) Images taken 175 days after initiating bevacizumab treatment. Marked tumor progression was evident by an increase in nonenhancing tumor (arrows in H) and with a small component of enhancing tumor (arrow in G) producing subfalcine herniation. After subtotal resection of the tumor on May 21, 2007, it was histologically proven to be glioblastoma.

Anti-VEGF Treatment in a Glioma Xenograft Model

To better understand the impact of anti-VEGF therapy on glioma biology, we developed an animal model that mimics the proinvasive effects of anti-VEGF treatments. Mice bearing intracranial U87 xenografts and treated with bevacizumab for 4–6 weeks developed a pattern of tumor invasion similar to that described previously.[21–23] Compared with IgG-treated controls, the bevacizumab-treated tumors had less vascular proliferation, as described previously. In contrast with the tumor cell localization in the human pathologic samples, in the mouse model, tumor cells were found to have spread along the perivascular space (Fig. 5C and D, white arrows) in areas adjacent to the tumor mass. U87 tumors also invaded along the subpial space, with tracking along Virchow–Robin spaces back into the brain (not shown). In striking contrast to the control-treated tumors (Fig. 5B), the tumors treated with bevacizumab had very invasive borders (Figs. 5C and 5D). This finding was similar to the invasive phenotype seen in the patient examples described above.

Immunohistochemical staining was performed in a parallel fashion as in the human cases, and expression patterns for factor VIII (Figs. 5C and 5D, white arrows) and MMP2 (Figs. 4C and 4D, black arrows) were strikingly similar to those in the patients' tumors.

Discussion

Antiangiogenic strategies for the treatment of high-grade gliomas have a strong biologic rationale since these tumors produce large amounts of VEGF and are highly vascular. The idea that antiangiogenic therapies normalize tumor vasculature has been eloquently demonstrated in patients with glioblastoma in a recent trial with the pan-VEGF receptor inhibitor cediranib. Batchelor et al.[11] showed that patients' tumors treated with cediranib exhibited a decrease in contrast enhancement with a concomitant decrease in vessel surface area and vessel permeability on MRI. Preliminary analyses of tumor tissue obtained from patients treated in that study showed a decrease in vessel density and restoration of
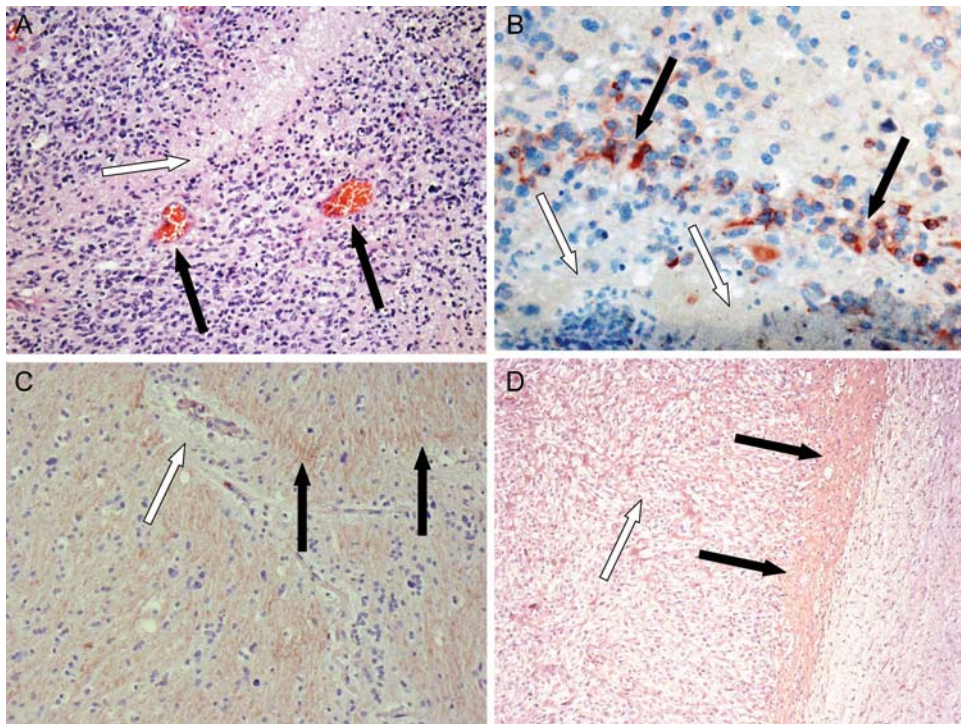
Fig. 4. Results of stereotactic biopsy of nonenhancing areas for case 3. (A and B) Human tumor samples from case 3 after progression during bevacizumab treatment. (A) Clearly visible areas of tumor necrosis (white arrow) and single endothelial cell walled vessels (black arrows). ×10 magnification. (B) Noted were areas of necrosis (white arrows), which were adjacent to areas that were positive for immunohistochemical staining for IGFBP2 (black arrows). ×40 magnification. (C and D) Immunohistochemical staining for MMP2 after treatment with bevacizumab. (C) In this specimen from case 3, the vasculature was composed of single endothelial cells (white arrow). Next to these vessels, an increase in expression of MMP2 was seen (black arrows). ×10 magnification. (D) In contrast, in the mouse U87 orthotopic xenograft model, cellular areas that were more dense (white arrow) and the leading edge (black arrows) were seen, which showed prominent staining for MMP2 (black arrows). ×5 magnification.

single endothelial cell walled vessel architecture and blood-brain barrier integrity, as measured by CD71 expression.[24] Similar changes in vasculature observed on MRI, with an attendant reduction in circulating VEGF levels, have been reported in patients with recurrent glioblastoma who received bevacizumab.[17] However, the histologic and vascular findings at the time of bevacizumab treatment failure have not been reported previously. Although clinical progression occurs coincident with FLAIR-indicated progression on MRI, this report is the first to demonstrate that the FLAIR changes are due to tumor infiltration. Perivascular tumor invasion was present in our preclinical model, but we did not observe this invasive pattern in the human cases. We show for the first time evidence of vascular normalization despite ongoing tumor progression and identify IGFBP2 and MMP2 as 2 potential mediators of the increased infiltrative pattern commonly observed on MRI.

The unusual pattern of tumor progression depicted in these cases is not typical of the radiographic pattern of glioblastoma progression, which normally emerges as both an increase in contrast-enhancing tumor as well as an increase in infiltrative disease with accompanying vasogenic edema. Several groups have observed that patients who receive anti-VEGF therapy have tumor

progression that is non−contrast-enhancing. In one recent study, there was a nonsignificant trend toward an increase in nonenhancing tumor progression in patients treated with bevacizumab compared with those treated with nonantiangiogenic therapy.[13] Continuous blockade of VEGF-induced vascular proliferation may promote tumor "escape" through vascular co-option, which may radiographically manifest itself as infiltrative, nonenhancing FLAIR progression. Although in our patients the areas of FLAIR progression were concordant with histologic evidence of recurrent infiltrative tumor, perivascular tumor invasion was not evident in the patients' pathologic samples.

There are many potential explanations for the discrepancy in perivascular invasion between the human cases and our animal model. First, this type of tumor escape may have been present but may not have been found because of sample bias. Alternatively, perivascular tumor invasion may be an early mechanism of tumor escape and a less prominent pathologic feature as the tumor progresses and utilizes multiple concurrent mechanisms of invasion. Third, glioma tumors may use vessel co-option early to escape the effects of continuous VEGF sequestration and at later stages the tumor may sustain angiogenesis via alternative growth factor pathways. Finally, glioma tumors are highly invasive at baseline,
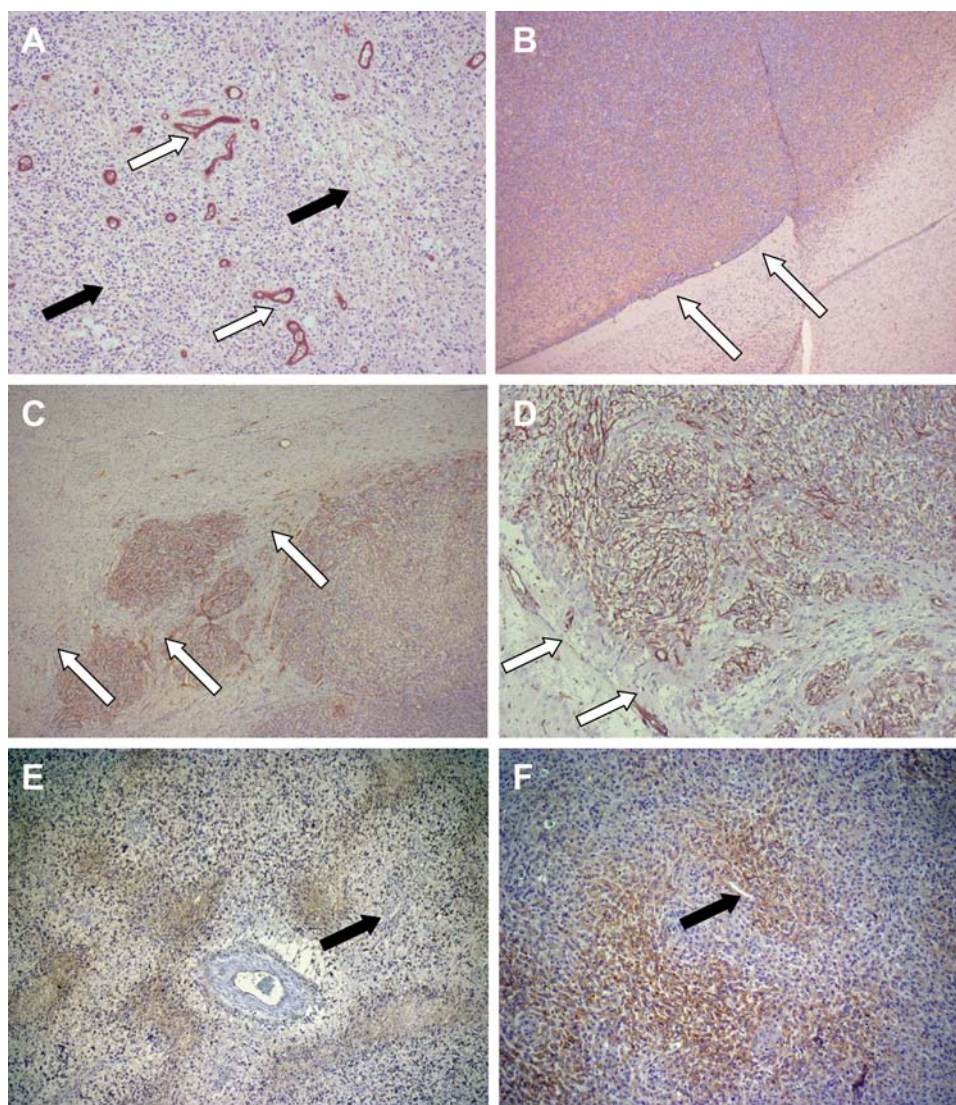
Fig. 5. Comparison of effects of anti-VEGF treatment between human and animal specimens. (A) In the tissue from case 3, single endothelial cell wall vasculature was clearly highlighted after staining for factor VIII ($\times 5$ magnification). (B–D) The U87 orthotopic xenograft model demonstrated striking changes after bevacizumab treatment. (B) Hematoxylin and eosin staining ($\times 2.5$ magnification) demonstrated typical (control) growth of U87 cells in the mouse brain, with a sharply defined leading edge of the tumor (white arrows). (C) In contrast, in animals treated with bevacizumab, tumor growth was infiltrative in nature ($\times 2.5$ magnification). Factor VIII staining highlighted the robust clusters of vessels in the infiltrating tumor. (D) A higher magnification ($\times 10$) of this infiltrating leading edge of the mouse xenograft tumor. Particularly important are the extension and infiltration of tumor cells beyond the dense vasculature (white arrows). The perivascular invasion noted in C and D contrasted with the more infiltrative growth pattern seen in the human tumor samples. CA9 staining in human (E) and U87 xenograft (F) tumor tissue. Prolonged, continuous antiangiogenic treatment significantly increased CA9 staining in tumor. Note the areas of necrosis and hypoxia adjacent to single endothelial cell vasculature (black arrows) and the dilated vessel with surrounding fibrosis.

and the forced invasion from anti-VEGF therapy may promote multiple types of tumor invasion, including the more typical neuropil infiltration.

That chronic anti-VEGF therapy both maintains vascular normalization and promotes tumor invasion has profound implications for the treatment of glioblastoma. It demonstrates that effective blocking of the vascular component of the tumor is insufficient for tumor control because the nonenhancing infiltrative component of the tumor is able to escape and to continue to infiltrate the CNS "behind" the blood-brain barrier. Newer agents that can effectively cross the blood-brain barrier would be logical candidate drugs to add to the combination of bevacizumab and irinotecan. Tumor cells may adapt to the reduced ability to stimulate neovascularization by co-opting the normal vasculature and occupying the perivascular niche. It is interesting to speculate that the perivascular niche may add to the treatment resistance of these infiltrative cells, as has been suggested for glioma tumor stem cells.[25] In this

way, tumor cells may be better able to sustain their nutrition and energy requirements. This progressive and resistant phenotype is difficult to treat, suggesting that these tumor cells are capable of progressing even when effective antiangiogenic therapy is being applied. Our experience and that of others are that there are currently no effective therapies that can block this tumor infiltration.[13] Since MMP expression around blood vessels has been implicated in the normalization process after anti-VEGF therapy,[16] and Src expression regulates MMP2 release,[26] Src inhibitors may have a role in the inhibition of anti–VEGF-induced invasion.

One of the most striking findings in our study was the pathologic finding that "normal"-appearing tumor vessels (single endothelial cell walled vessels) existed adjacent to areas of tumor necrosis. Typically, an area of tumor necrosis is induced by rapidly growing tumor, which depletes nutrients and oxygen, ultimately resulting in tumor hypoxia. This hypoxia leads to increased VEGF production and ensuing florid vascular proliferation. It has been suggested that antiangiogenic therapy leads to vascular normalization, with the expected consequence of improving oxygen delivery and potentially increasing drug delivery to tumor.[14,27] These changes are expected to occur within a transient "window" of time.[14] However, long-term antiangiogenic treatments may also lead to an increase in tumor hypoxia[28] as suggested by the profound CA9 staining seen in our bevacizumab-failure cases, presumably due to a decrease in tumor oxygenation, which has been shown to increase tumor invasion in animal models.[22] The resultant decrease in blood flow may also decrease nutrient delivery, placing additional physiologic stress on the tumor, which may contribute to the phenotypic shift of the tumor becoming more invasive. Furthermore, antiangiogenic agents may decrease drug delivery to glioblastoma tumors,[29,30] which could be one reason for the lack of efficacy of changing the chemotherapy regimen for patients whose disease progresses during bevacizumab treatment. Finally, during prolonged periods of anti-VEGF therapy, alternative mechanisms of angiogenesis involving fibroblast growth factor, platelet-derived growth factor, and other endothelial growth factors may partially reconstitute the vasculature and ameliorate oxygen and nutrient stress.[11,31,32] Fibroblast growth factor has been shown to be important in the migration and invasion of some tumors,[33] and an increase in its expression during VEGF blockade could lead to a similar effect in glioma.

The pathologic findings described in this report have critical implications for the care of patients with recurrent glioblastoma. A better understanding of the biologic basis leading to these pathologic changes is essential and may provide key insights into approaches to improving the overall survival of these patients. If IGFBP2 and MMP2 are confirmed to be molecular mediators of tumor evasion of anti-VEGF therapy, then combination strategies can be designed to inhibit these targets. Better methods of predicting which patients are likely to develop these changes and improved radiologic measures for detecting tumor invasion are also important in improving care for patients receiving antiangiogenic therapy. Our animal model that simulates the human clinical scenario will be a useful tool as we dissect the causes of and develop effective treatment strategies for these unintended consequences of antiangiogenic therapy.

References

1. Stupp R, Mason WP, van den Bent MJ, et al. Radiotherapy plus concomitant and adjuvant temozolomide for glioblastoma. *N Engl J Med*. 2005;352:987–996.

2. Wong ET, Hess KR, Gleason MJ, et al. Outcomes and prognostic factors in recurrent glioma patients enrolled onto phase II clinical trials. *J Clin Oncol*. 1999;17:2572–2578.

3. Curran WJ, Jr, Scott CB, Horton J, et al. Recursive partitioning analysis of prognostic factors in three Radiation Therapy Oncology Group malignant glioma trials. *J Natl Cancer Inst*. 1993;85:704–710.

4. Millauer B, Shawver LK, Plate KH, Risau W, Ullrich A. Glioblastoma growth inhibited in vivo by a dominant-negative Flk-1 mutant. *Nature*. 1994;367:576–579.

5. Folkman J. Tumor angiogenesis. *Adv Cancer Res*. 1985;43:175–203.

6. Folkman J. Angiogenesis in cancer, vascular, rheumatoid and other disease. *Nat Med*. 1995;1:27–31.

7. Parangi S, O'Reilly M, Christofori G, et al. Antiangiogenic therapy of transgenic mice impairs de novo tumor growth. *Proc Natl Acad Sci USA*. 1996;93:2002–2007.

8. Stark-Vance V. Bevacizumab and CPT-11 in the treatment of relapsed malignant glioma [abstract]. Proceedings of the World Federation of Neuro-Oncology Meeting. *Neuro-Oncology*. 2005;7:369.

9. Vredenburgh JJ, Desjardins A, Herndon JE, 2nd, et al. Phase II trial of bevacizumab and irinotecan in recurrent malignant glioma. *Clin Cancer Res*. 2007;13:1253–1259.

10. Wagner SA, Desjardins A, Reardon DA, et al. Update on survival from the original phase II trial of bevacizumab and irinotecan in recurrent malignant gliomas [abstract]. *J Clin Oncol*. 2008;26:abstract 2021.

11. Batchelor TT, Sorensen AG, di Tomaso E, et al. AZD2171, a pan-VEGF receptor tyrosine kinase inhibitor, normalizes tumor vasculature and alleviates edema in glioblastoma patients. *Cancer Cell*. 2007;11:83–95.

12. Cloughesy TF, Prados MD, Wen PY, et al. A phase II, randomized, non-comparative clinical trial of the effect of bevacizumab (BV) alone or in combination with irinotecan (CPT) on 6-month progression free survival (PFS6) in recurrent, treatment-refractory glioblastoma (GBM) [abstract]. *J Clin Oncol*. 2008;26:abstract 2010b.

13. Norden AD, Young GS, Setayesh K, et al. Bevacizumab for recurrent malignant gliomas: efficacy, toxicity, and patterns of recurrence. *Neurology*. 2008;70:779–787.

14. Jain RK. Normalization of tumor vasculature: an emerging concept in antiangiogenic therapy. *Science*. 2005;307:58–62.

15. Willett CG, Boucher Y, di Tomaso E, et al. Direct evidence that the VEGF-specific antibody bevacizumab has antivascular effects in human rectal cancer. *Nat Med*. 2004;10:145–147.

16. Winkler F, Kozin SV, Tong RT, et al. Kinetics of vascular normalization by VEGFR2 blockade governs brain tumor response to radiation: role of oxygenation, angiopoietin-1, and matrix metalloproteinases. *Cancer Cell*. 2004;6:553–563.

17. Desjardins A, Barboriak DP, Herndon JE, II, et al. Effect of bevacizumab (BEV) and irinotecan (CPT-11) on dynamic contrast-enhanced magnetic resonance imaging (DCE-MRI) in glioblastoma (GBM) patients [abstract]. *J Clin Oncol*. 2008;26:abstract 2026.

18. Macdonald DR, Cascino TL, Schold SC, Jr, Cairncross JG. Response criteria for phase II studies of supratentorial malignant glioma. *J Clin Oncol*. 1990;8:1277–1280.

19. Lal S, Lacroix M, Tofilon P, Fuller GN, Sawaya R, Lang FF. An implantable guide-screw system for brain tumor studies in small animals. *J Neurosurg*. 2000;92:326–333.

20. Wang H, Wang H, Shen W, et al. Insulin-like growth factor binding protein 2 enhances glioblastoma invasion by activating invasion-enhancing genes. *Cancer Res*. 2003;63:4315–4321.

21. Lamszus K, Kunkel P, Westphal M. Invasion as limitation to anti-angiogenic glioma therapy. *Acta Neurochir Suppl*. 2003;88:169–177.

22. Du R, Lu KV, Petritsch C, et al. HIF1alpha induces the recruitment of bone marrow-derived vascular modulatory cells to regulate tumor angiogenesis and invasion. *Cancer Cell*. 2008;13:206–220.

23. Rubenstein JL, Kim J, Ozawa T, et al. Anti-VEGF antibody treatment of glioblastoma prolongs survival but results in increased vascular cooption. *Neoplasia*. 2000;2:306–314.

24. diTomaso E, Frosch MP, Auluck PK, et al. Characterization of blood vessels in brain autopsies of GBM patients who received antiangiogenic treatment [abstract]. *J Clin Oncol*. 2008;26:abstract 2009.

25. Sakariassen PO, Prestegarden L, Wang J, et al. Angiogenesis-independent tumor growth mediated by stem-like cancer cells. *Proc Natl Acad Sci USA*. 2006;103:16466–16471.

26. Park CM, Park MJ, Kwak HJ, et al. Ionizing radiation enhances matrix metalloproteinase-2 secretion and invasion of glioma cells through Src/epidermal growth factor receptor-mediated pp38/Akt and phosphatidylinositol 3-kinase/Akt signaling pathways. *Cancer Res*. 2006;66:8511–8519.

27. Jain RK. Normalizing tumor vasculature with anti-angiogenic therapy: a new paradigm for combination therapy. *Nat Med*. 2001;7:987–989.

28. Casanovas O, Hicklin DJ, Bergers G, Hanahan D. Drug resistance by evasion of antiangiogenic targeting of VEGF signaling in late-stage pancreatic islet tumors. *Cancer Cell*. 2005;8:299–309.

29. Zhou Q, Guo P, Gallo JM. Impact of angiogenesis inhibition by sunitinib on tumor distribution of temozolomide. *Clin Cancer Res*. 2008;14:1540–1549.

30. Ma J, Pulfer S, Li S, Chu J, Reed K, Gallo JM. Pharmacodynamic-mediated reduction of temozolomide tumor concentrations by the angiogenesis inhibitor TNP-470. *Cancer Res*. 2001;61:5491–5498.

31. Dong J, Grunstein J, Tejada M, et al. VEGF-null cells require PDGFR alpha signaling-mediated stromal fibroblast recruitment for tumorigenesis. *Embo J*. 2004;23:2800–2810.

32. Willett CG, Boucher Y, Duda DG, et al. Surrogate markers for antiangiogenic therapy and dose-limiting toxicities for bevacizumab with radiation and chemotherapy: continued experience of a phase I trial in rectal cancer patients. *J Clin Oncol*. 2005;23:8136–8139.

33. Fischer H, Taylor N, Allerstorfer S, et al. Fibroblast growth factor receptor-mediated signals contribute to the malignant phenotype of non-small cell lung cancer cells: therapeutic implications and synergism with epidermal growth factor receptor inhibition. *Mol Cancer Ther*. 2008;7:3408–3419.